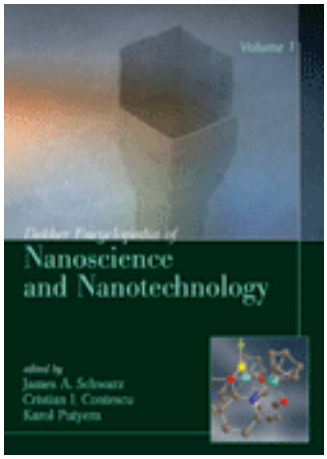

Dekker Encyclopedia of Nanoscience and Nanotechnology
Publication details, including instructions for authors and subscription information:
http://www.informaworld.com/smpp/title~content=t713172968

Magnetic Nanoparticles for Biomedical Applications: Synthesis, Characterization and Uses

Nguyen T. K. Thanh [a]; Ian Robinson [a]; Le D. Tung [b]
[a] Centre for Nanoscale Sciences, Department of Chemistry and School of Biological Sciences, University of Liverpool, Liverpool, U.K.
[b] Department of Physics, University of Warwick, Coventry, U.K.

Online Publication Date: 20 December 2007
To cite this Section: Thanh, Nguyen T. K., Robinson, Ian and Tung, Le D. (2007) 'Magnetic Nanoparticles for Biomedical Applications: Synthesis, Characterization and Uses', Dekker Encyclopedia of Nanoscience and Nanotechnology, 1:1, 1 - 10
To link to this article: DOI: 10.1081/E-ENN-120042172
URL: http://dx.doi.org/10.1081/E-ENN-120042172

Magnetic Nanoparticles for Biomedical Applications: Synthesis, Characterization and Uses

Nguyen T.K. Thanh
Ian Robinson
Centre for Nanoscale Sciences, Department of Chemistry and School of Biological Sciences, University of Liverpool, Liverpool, U.K.

Le D. Tung
Department of Physics, University of Warwick, Coventry, U.K.

Abstract
The synthesis, characterization, and some aspects of biomedical applications of the magnetic nanoparticles are reviewed. We will be focusing on some of the most common chemical methods and experimental techniques to synthesize and characterize the magnetic nanoparticles. The mechanism in which the magnetic nanoparticles are to be used in some biomedical applications, such as magnetic separation, targeted drug delivery, hyperthermia cancer treatment, and MRI contrast agents, is also explored.

INTRODUCTION

Interest in nanoparticles has grown rapidly in recent years because of their diverse applications in biomedicine and as novel materials for engineering and devices. Magnetic nanoparticles are of particular interest because of their potential application in areas such as magnetic separation, magnetic resonance imaging (MRI), targeted drug delivery, hyperthermia treatment of solid tumors, and high-density magnetic storage.

In this article, we cover some of the synthesis methods (chemical reduction in reverse micelle, and solution, fabrication in hydrogels, thermal decomposition, seed-mediated growth, and precipitation from aqueous solution) and characterization of magnetic nanoparticles (transmission electron microscopy (TEM), X-ray diffraction (XRD), X-ray absorption spectroscopy (XAS), superconducting quantum interference device (SQUID), Mössbauer spectroscopy, and small angle neutron scattering (SANS). We will also explore some of the biomedical applications such as magnetic separation, targeted drug delivery, hyperthermia cancer treatment, and MRI contrast agents.

METHODS OF SYNTHESIS

Fabrication of nanoparticles can be grouped into three main synthetic methods: solid, gas, and solution.[1] The solid route involves the mechanical milling or the mechanochemical synthesis of raw powder to produce nanoparticles. This method has the disadvantage of introducing contamination to the products from the milling equipment as well as producing particles with wide size distribution. In gas and chemical routes, the synthesis can be considered as either ''phase-transformation'' or ''phase-build-up.'' The ''phase-transformation'' can be described as the conversion of finely divided metal compounds into metals through thermal decomposition (see later) or chemical reduction. On the other hand, in ''phase-build-up,'' particles are ''constructed'' from building blocks (metal atoms). This process can take place from the gas phase (chemical or physical vapor deposition) or from the liquid phase (chemical precipitation). Gas-phase synthesis involves the formation of a supersaturated vapor of condensable gaseous species as a result of a chemical reaction that produces a new species or as a result of a physical process such as cooling that will reduce the vapor pressure of the condensable species. There are also several methods that use the solution route and are discussed in further detail later. These techniques produce uniform nanoparticles of different shapes by using appropriate precursors and by adding a surfactant or a capping ligand during the transformation. The addition of a surfactant/capping ligand can also prevent aggregation of the particles.

In the liquid phase, the chemical precipitation usually occurs from homogeneous solution. When the concentration of the constituent precursor reaches critical supersaturation, there is short burst of nucleation. This is followed by a period of uniform growth as the solutes diffuse from the solution to the surface of the nuclei until the final size is reached. To achieve monodisperse nanoparticles, this process requires the separation of the nucleation and growth phases, with no further nucleation occurring during the growth period. Multiple nucleation events can result in small

Dekker Encyclopedia of Nanoscience and Nanotechnology DOI: 10.1081/E-ENN-120042172

particles aggregating to form much larger particles.[2,3] This process is known as Ostwald ripening and typically leads to the coarsening of the size distribution of the particles. Nucleation, particle growth, and particle interaction can be better controlled in a liquid medium, making chemical precipitation a more favorable method for producing uniform particles with well-controlled features (see Fig. 1).

Chemical Reduction in Solution

Reduction is the transfer of electrons from reducing agent to oxidized metal species in a process driven by redox potential of the reaction, ΔE^0. The value of ΔE^0 will indicate the likelihood of the reduction proceeding and can predict the rate of the chemical reaction. An increase in its value is associated with faster generation of atoms in the liquid phase. This leads to a higher supersaturation concentration of atoms and therefore faster nucleation. Thus, finely controlling the redox potential of the reacting species and the overall reaction is vitally important in controlling the properties of the metal particle produced. Complexing or precipitating the oxidized metallic species can alter their electrochemical potential. The degree of change is dependent on the stability constants or the solubility products of the resulting compounds.[4]

The reducing agent can form an intermediate with the oxidized metal species without altering its oxidation state. In this situation, the reduction process can be initiated by increasing the temperature, for example, and it can be conducted very slowly, producing conditions that lead to the formation of highly crystalline structures of regular shape.

An example of this is the reduction of iron (II) chloride and platinum acetylacetonate using superhydride ($LiBEt_3H$) at high temperature (263°C) to produce 4 nm FePt magnetic nanoparticles.[5] Alternatively, 5 nm CoPt nanoparticles can be produced by coreduction of cobalt and platinum acetylacetonate in trimethylene glycol.[6] These particles are ferromagnetic at room temperature and by annealing above 550°C, the magnetic properties of the nanoparticles can be enhanced, owing to the induction of ordering.

Redox Transmetallation

This process involves metal ions of the reactant metal complexes being reduced on the surface of metal (Me) nanoparticles with the simultaneous oxidation of the neutral Me^0 to Me^{n+} via ligand migration to form a metal–ligand complex as a reaction by-product.[7–9] This process also means that the particle size remains the same during the reaction. Using redox transmetallation, Lee et al.[9] fabricated cobalt core nanoparticles with shells of gold, palladium, platinum, and copper. Of particular interest are Co@Au core-shell nanoparticles, because they can be transferred to the aqueous phase without losing any magnetism and the gold shell layer is very versatile.[9]

Reduction in Reverse Micelles

Reverse micelles are spherical aggregates formed by surfactants dissolved in organic solvent. In the presence of small amount of water, which is readily solubilized in the polar core, monodisperse aggregates can be formed.[10] In contrast, microemulsions are formed with a larger amount of water. The reverse micelles can be used as microreactors for the synthesis of nanoparticles. Briefly, aqueous solutions of metal salts

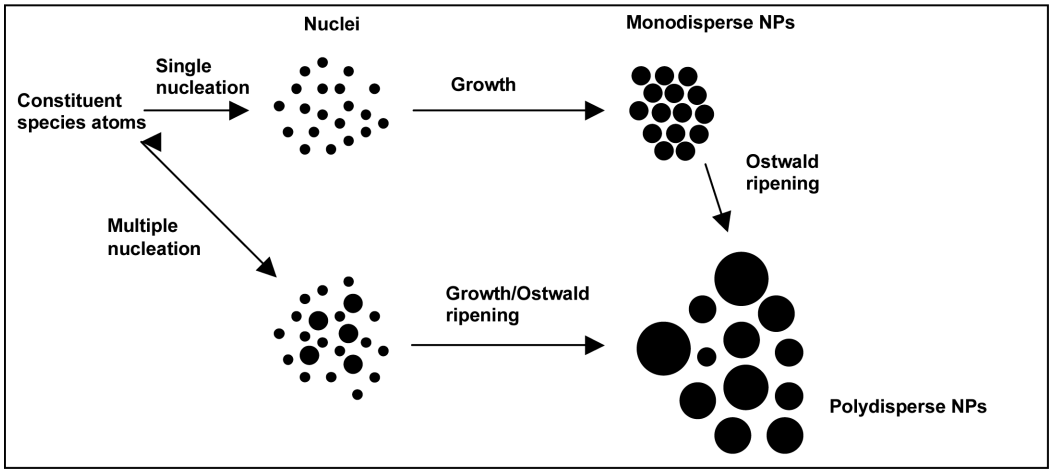

Fig. 1 Formation mechanism of nanoparticles where, following a single burst of nucleation, a period of uniform growth leads to the formation of monodisperse nanoparticles by diffusion. Multiple nucleation events and growth via Ostwald ripening can lead to polydisperse suspensions of nanoparticles.

containing elements that formed the desired nanoparticle are added to the reverse micelle suspension. A reductant (e.g., $NaBH_4$) is added to the mixture and once the metallic nanoparticles are formed, the micelle solution is disrupted by the addition of an excess amount of polar solvent (e.g., $CHCl_3$: methanol) and the particles are collected.[11–15]

Reverse micelles provide unique reaction media as they can solubilize, concentrate, localize, and even organize reactants. They also allow the nanoparticle synthesis to take place in aqueous solution. However, control of the size and shape of nanoparticles synthesized by this method is difficult as it reflects the interior of the micelles.

Hydrogels

A hydrogel is a gel that will expand greatly in aqueous solution. They are usually composed of a hydrophilic organic polymer component that is cross-linked through either covalent or non-covalent interactions.[16] They can be synthesized to contain magnetic nanoparticles by using a two-step emulsifier-free emulsion polymerization. For example, bovine serum albumin (BSA) can be covalently attached to the particles to form thermosensitive magnetic immunospheres, which can be very useful in the immunoaffinity purification of anti-BSA antibodies from antiserum.[17]

Thermal Decomposition

In this process, organometallic complexes are rapidly broken down in hot solvent containing surfactant, which can form a protecting layer around the nanoparticle, whilst acting as a dispersant. For example, the rapid pyrolysis of $Co_2(CO)_8$ in *o*-dichlorobenzene, in the presence of trioctyl phosphine oxide (TOPO) and oleic acid at 185°C will produce cobalt nanoparticles, whose size and shape can be controlled by varying the molar ratios of precursor and surfactant.[18,19] The protective layer can also consist of polymers, which can be tailored to improve the biocompatibility of the nanoparticles. For example, Stevenson et al.[20] used a poly[dimethylsiloxane-*b*-(3-cyanopropyl)methylsiloxane-*b*-dimethylsiloxane] (PDMS–PCPMS–PDMS) family of triblock polymers with controlled length to coat Co nanoparticles. The central block (PCPMS) is absorbed onto the nanoparticle surface and the hydrophobic end-blocks protrude into the carrier fluid (poly[dimethylsiloxane]), providing suspension stability. Alternatively, one can also use peptides as capping ligands for *in situ* synthesis of water-soluble Co nanoparticles with the aim to use these particles for biological applications.[21] The ability to tune the properties of the peptides (by varying the length, and sequence of amino acids) makes them a unique class of ligands for combinatorial nanomaterial synthesis. In addition to the 20 amino acids that occur naturally in proteins, over 100 unnatural amino acids are available for peptide synthesis, which provide access to a huge chemical combinatorial space. Like metallic nanoparticles, 13 nm monodisperse maghemite particles have been synthesized by injecting $Fe(CO)_5$ into a solution containing surfactants and a mild oxidant (trimethylamine oxide).[22] Moreover, Park et al.,[23] using the same method, have been able to synthesize monodisperse iron oxide nanoparticles with extremely fine size control, producing particles with diameters of 6, 7, 9, 10, 12, 13, and 15 nm.

Seed-Mediated Growth

Introducing ''seeds'' to a reaction mixture can increase the nucleation rate and thus the properties of the resulting nanoparticles.[4] The catalytic or surface properties of the small solid entities can trigger the reduction of the species and the nucleation process. This is of particular use in systems in which nucleation would otherwise not take place or would be too slow. It also has the advantage of artificially separating the nucleation and growth phases of the particle formation.

Seeds can be produced ''in situ'' by the rapid reduction of a different, more electropositive element or be in the form of a stable dispersed preformed nanosized particle of the same element. To form monodisperse nanoparticles, it is necessary for the nucleation process to be uniform throughout the entire solution, a condition that is difficult to achieve in rapid reductions. This has an effect upon reproducibility and scale up of the process.

To avoid this, it is favorable to use systems in which the electron transfer is inhibited when the reactant species are brought into contact, but can be induced by changing the conditions (e.g., pH, temperature, etc.) after the system is already homogenized. For example, the solvent used to dissolve the metal salts will become the reducing agent on changing the conditions. Wang et al.[24] used Fe_3O_4 nanoparticles as seeding materials for the reduction of gold precursors to synthesize gold-coated Fe_3O_4 nanoparticles (Fe_3O_4@Au).

Precipitation from Aqueous Solution

Precipitation routes from aqueous solution are widely used for the synthesis of iron oxide nanoparticles.[25] One method involves ferrous hydroxide suspensions

that are partially oxidized, using a variety of oxidizing agents. The amorphous ferrous hydroxide is first precipitated and the aqueous gel is aged at 90°C over various time periods in the presence of a mild oxidant (e.g., nitrate ions). A study of the evolution of the precipitation with time has shown that minute primary particles, nucleated in the ferrous hydroxide gel, aggregate and then larger particles form by a contact-recrystallization mechanism. The aggregation of the primary iron oxide particles results from the Van der Waals and magnetic forces acting under the conditions of week repulsion, close to the isoelectric point, giving rise to spherical crystalline particles.[26]

An example of this is using an iron (II) chloride and iron (III) nitrate mixture (at a ratio of 1 : 1) in a basic aqueous solution to precipitate spherical magnetite (Fe_3O_4) nanoparticles with an average diameter of 7 nm.[27] Alternatively, by adding polyelectrolytes, again at basic pH, to the iron salts during the precipitation, ferrite nanoparticles of nearly uniform size can be produced.[28] By varying the polyelectrolyte concentration in the solution, the size of the resulting iron oxide nanoparticles can be easily controlled.

CHARACTERIZATION METHODS

For sample characterization, it is important to know the phase, morphology (size and shape), as well as the physical properties of the as-prepared magnetic nanoparticles. In the following, we will cover some of the most common techniques for this purpose.

Phase and Morphology Characterization

Transmission electron microscopy

Transmission electron microscopy (TEM) is one of the most common techniques used to visualize and determine the morphology of the particles. In this technique, the specimen is illuminated by a beam of monochromatic electrons, some of which are transmitted through the objective lens and then projected onto a viewing screen (for example, a layer of electron fluorescent material) to produce an image. In TEM, one can "see" particles as small as a few angstroms (10^{-10} m), which is near atomic levels. As an example, in Fig. 2 is shown the TEM image of a self-assembled sample of Co nanoparticles with the mean particle size of 4.5 nm; the particle size distribution is also shown in the left panel.

High-resolution transmission electron microscopy (HRTEM) can sometimes be used for complex structures such as core-shell or those consisting of an alloy. The HRTEM allows us to obtain information on the crystal planes of the particles and measure the lattice distance.

Scanning electron microscopy

A scanning electron microscope (SEM), like TEM, uses a beam of electrons aimed at a specimen; therefore, both instruments have similar features such as an electron gun, condenser lenses, and a vacuum system. However, the images are produced and magnified in different ways and while TEM provides information about the morphology of the nanoparticles, SEM is

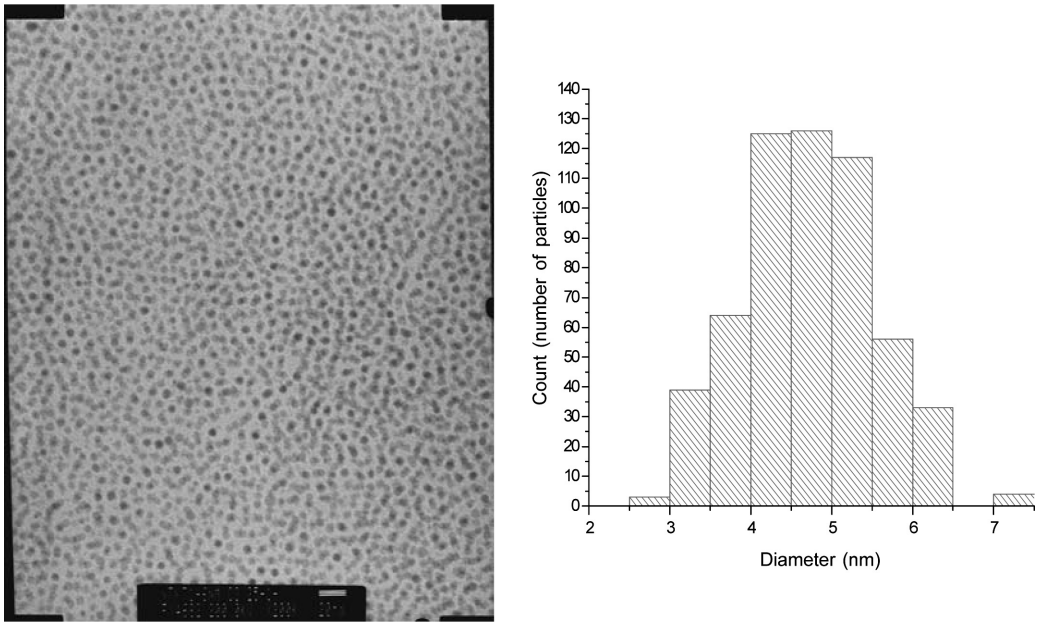

Fig. 2 TEM micrograph of 4.5 nm Co nanoparticles with the size distribution graph (Bar 50 nm).

mainly used to study the surface or near surface structure of bulk specimens. The spatial resolution of SEM is approximately 15 nm, and therefore, not as good as TEM, which can have spatial resolutions in the subnanometer range; however, SEM images are generally much easier to interpret. Also SEM has the ability to image a comparatively large area of the specimen; the ability to image bulk materials (not just thin films or foils); and the variety of analytical modes available for measuring the composition and nature of the specimen.

Field-emission SEM (FESEM) uses a field-emission cathode in the electron gun of a scanning electron microscope and provides narrower probing beams both at low and high electron energy; this results in both improved spatial resolution and minimized sample charging and damage. FESEM produces clearer, less electrostatically distorted images with spatial resolution down to 1.5 nm or better, i.e., several times better than the conventional SEM. High-quality, low-voltage images are obtained with negligible electrical charging of samples (accelerating voltages range from 0.5 to 30 kV).

X-ray diffraction

Powder X-ray diffraction (XRD) is the most conventional technique that can be used to determine the structure, phases, and average size of the particles. In this technique, the structure and the lattice parameters are determined by fitting the X-ray patterns by means of the Rietveld profile procedure;[29] several software programs are available, such as FULLPROF.[30] The size of the particles can also be determined from the width of the X-ray peaks using the Scherrer formula.[31] The particle size estimated from the XRD is often found to be larger than that from TEM estimates because of the broadening of X-ray diffraction lines, which can be affected by many factors. In addition, the X-ray coherence length does not allow the technique to be applied to the study of particles that are too small (say less than 1 nm).

X-ray absorption spectra

When a beam of X-rays passes a sample, it can be absorbed. A certain amount of energy of the incident X-ray photons is sufficient to cause excitation of a core electron of an absorbing atom, which causes it to pass into a continuum state, thus producing a photoelectron. This results in a drastic increase in the absorption, giving rise to an absorption edge. If one defines the electron binding energy as E_0, an X-ray absorption spectrum (XAS) is generally divided into four sections: (1) pre-edge ($E < E_0$); (2) X-ray absorption near edge structure (XANES), where the energy of the incident X-ray beam is $E = E_0 \pm 10$ eV; (3) near edge X-ray absorption fine structure (NEXAFS), in the region between 10 eV up to 50 eV above the edge; and (4) extended X-ray absorption fine structure (EXAFS), which starts approximately from 50 eV and continues up to 1000 eV above the edge. The analysis of the different spectrum sections is particularly useful. The XANES contains information about the electronic state of the X-ray absorbing atom and the local structure around it. The NEXAFS can give information relating to bond angles, bond lengths, and the presence of adsorbates. Finally, the EXAFS can give information on the atomic number, distance, and coordination number of the atoms surrounding the element.

Magnetization Characterization

Magnetic particles with size smaller than few tens of nanometers can be considered as single magnetic domains, which display properties markedly different from the bulk. One of the interesting features of nanosize magnetic materials is the presence of the magnetic relaxation process that is due to the thermal effect and the existence of the energy barriers separating the local minima for different equilibrium states of the system. As a result, the magnetic behavior of a small particle depends on its relaxation time (τ),

$$\tau = \tau_0 \exp[KV/(k_B T)],$$

where τ_0 is of the order of 10^{-9}–10^{-13} s and weakly depends on temperature, k_B the Boltzmann constant, T the temperature; and K and V are the anisotropy and (average) volume of the particle, respectively. When τ is smaller than the experimental time window (τ_{ex}), the magnetization vector is seen to change quickly between different states, i.e., the system is in a superparamagnetic state. By contrast, when $\tau > \tau_{ex}$, , the thermal dynamic equilibrium state is very difficult to observe, since the energy barriers arising from the anisotropy obstruct the magnetization vector from switching to a lower energy state. This case is generally called the blocked state. The temperature at which $\tau = \tau_{ex}$ is defined as the blocking temperature.

For magnetization characterization, it is important to determine the blocking temperature of the nanoparticle sample. From this, sometimes one can also obtain complementary information such as the monodispersity of the sample; size and anisotropy of the particles; formation of an oxide layer on the intermetallic sample, and the magnetic (dipole–dipole) interaction between particles.

One of the most common devices used in magnetization characterization is the superconducting quantum interference device (SQUID) in which the magnetization can be measured within an experimental

window τ_{ex} of about 20 s. Here, one can determine the blocking temperature T_B of the sample from a standard zero-field-cooled (ZFC) and field-cooled (FC) measurement of the magnetization. As an example, Fig. 3 shows the results measured on 3.3 nm $CoFe_2O_4$ nanoparticles. The ZFC curve shows a peak at about 90.5 K, which corresponds to the blocking temperature T_B. This sample shows a good monodispersity with the sharp peak at T_B and the splitting between ZFC and FC curves occurs very close to the peak's position.

Another useful magnetization characterization can be realized on measuring the a.c. susceptibility at different frequencies (f). Here, the experimental time window $\tau_{ex} = 1/f$. Fig. 4 shows an example for 3.3 nm $CoFe_2O_4$ nanoparticles. It can be seen that the blocking temperature T_B at the peak of the a.c. susceptibility shifts toward higher temperatures with increasing frequencies. The slope of the plot $\ln \tau_{ex}$ vs. $1/T_B$ in the inset of Fig. 4 gives information on the anisotropy (K) and the volume of the particles (V) through the relationship $\ln \tau_{ex} = \ln \tau_0 + KV/k_BT_B$.[32]

Other Techniques for Characterization of Magnetic Nanoparticles

Mössbauer spectroscopy

Mössbauer technique is a very useful tool for probing the properties of materials although it can be applied only to those consisting of elements (more than 40) that are Mössbauer-active of which ^{57}Fe is the most prominent ''Mössbauer nuclide.'' For magnetic nanoparticles, the magnetic hyperfine field splitting in the Mössbauer spectra begins right below the blocking temperature T_B where the relaxation rate of particles has slowed down sufficiently for the reversal energy to exceed the thermal energy.[33] Note that because of very small experimental time window (τ_{ex}) in Mössbauer ($\approx 10^{-9}$ s) when compared with other techniques such as SQUID ($\approx$20 s), the blocking temperature derived from the technique is higher. The analysis of the spectra close to T_B would give information on the size distribution of the particles. Spectra below T_B can give different information on the phase(s) of the sample, oxidation state, magnetic structure, dynamics effects as well as the interaction between the particles.

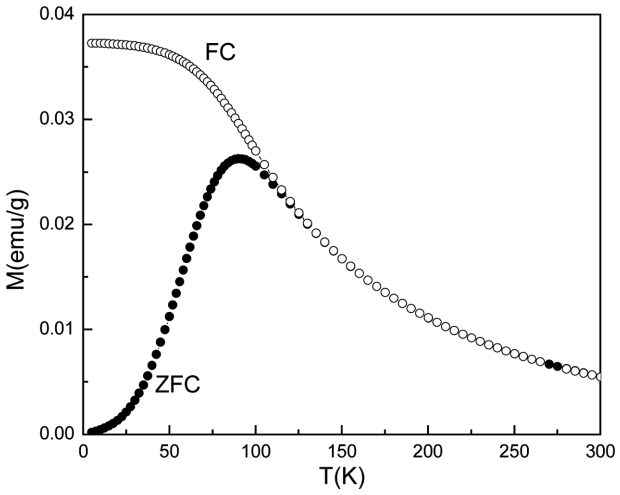

Fig. 3 Temperature dependence of the magnetization of 3.3 nm $CoFe_2O_4$ nanoparticles measured in zero-field cooled (ZFC) and field-cooled (FC) conditions with an applied field $H = 10$ Oe.

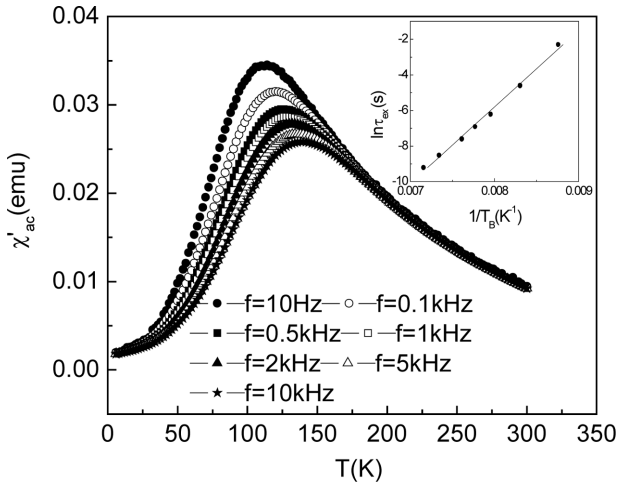

Fig. 4 Temperature dependence of the in-phase component of the a.c. susceptibility of 3.3 nm $CoFe_2O_4$ nanoparticles (χ'_{ac}) at different frequencies. The inset shows the logarithm of the experimental time window τ_{ex} as a function of inverse blocking temperature ($1/T_B$).

Small angle neutron scattering

Small angle neutron scattering (SANS) is a useful tool to study magnetic nanoparticles. In contrast to light and X-rays, which are scattered by the electrons surrounding atomic nuclei, neutrons are scattered by the nucleus itself. In this technique, one can ''see'' the particle in the range between 1 and 500 nm. Several parameters can be evaluated from SANS data, including the radius of gyration, the particle surface area, shape of the scattering particles, magnetic structure, magnetic correlation, alignment of nanoparticles as well as their response to an external magnetic field.[34,35]

BIOMEDICAL APPLICATIONS

Magnetic Separation

Since magnetic nanoparticles can be quickly separated by magnetic forces, they are excellent candidates for

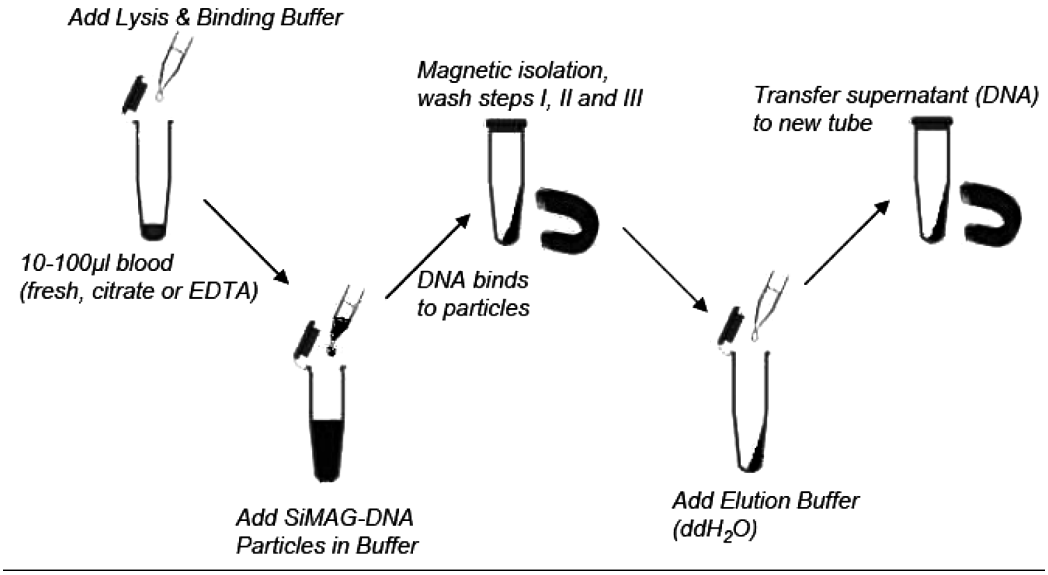

Fig. 5 Schematic view of the use of magnetic nanoparticles to separate the DNA from blood sample. *Source*: From http://www.chemicell.com.

purification and reuse in biotechnology. The special advantages of magnetic separation techniques are the fast and simple handling of a sample vial and the opportunity to deal with large sample volumes. This is because intensive steps of centrifugation can be omitted. Therefore, biomagnetic separation is highly compatible for labor automatization systems that will play a very important role in the near future.

In magnetic separation, first the magnetic nanoparticles have to be tagged with a desired biological entity such as proteins, DNA, RNA, enzymes, blood cells, and cancer cells in the native solution. This tagging can be made possible by chemical coating of magnetic nanoparticles with biocompatible molecules such as dextran, peptides, and phosopholipids. The magnetically labeled entities can then be separated using a permanent magnet and washed with water. Finally, the magnetic particles can be untagged and removed again by a magnetic field to obtain the desired biological product. An example of the use of magnetic nanoparticles for the separation of DNA from a blood sample is illustrated in Fig. 5.

Drug Delivery

Most current chemotherapies are relatively nonspecific and tend to attack normal healthy tissue leading to unwanted side effects that can lead to the discontinuation of their use. However, if such treatments could be localized, e.g., anti-inflammatory drug to arthritic joints, the dose and thus the side effects could be minimized allowing prolonged use of these agents (see Fig. 6).[36]

One particular method of achieving this would be to attach a therapeutic drug to a biocompatible magnetic nanoparticle carrier that is injected into the patient via the circulatory system. Once in the blood stream, the drug-carrier complex can be concentrated at a specific site by applying a high-gradient, external magnetic field; the drug released via enzymatic activity or changes in the physiological conditions.[37]

There are several physical parameters that govern the effectiveness of the therapy, including field strength, gradient, and volumetric and magnetic properties of the particles. Hydrodynamic factors, such as blood flow rate, carrier concentration, and infusion

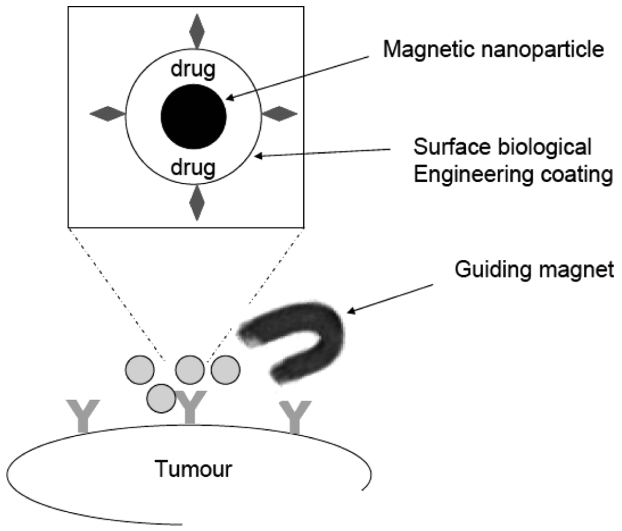

Fig. 6 Schematic view of the use of magnetic nanoparticles for guided drug delivery.

route and circulation time, will also play a major role if the carriers are administered via the circulatory system. Finally, physiological parameters such as tissue depth to the target site (i.e., distance from the magnetic field source), reversibility, and strength of the drug/carrier binding and, in cancer treatments, tumor volume are also very important.[38]

Generally, the carriers are magnetic particles coated with a biocompatible molecule (e.g., polymer, peptide, silica), which can be functionalized by adding carboxyl groups, biotin, avidin, and other molecules.[39–41] These molecules can then act as attachment points for the coupling of therapeutic drugs.[42]

Therapeutic Hyperthermia

Hyperthermia treatment of cancers involves using a device to heat malignant cells. However, the majority of devices are restricted in their use owing to coincidental damage to surrounding healthy tissue. Magnetic nanoparticle hyperthermia provides a possible solution to this problem. Generally, magnetic particles can be dispersed into the target tissue and an AC magnetic field of sufficient strength and frequency is applied resulting in the heating of the particles. The heat is then transferred to the surrounding diseased tissue and if the temperature can be maintained above the therapeutic threshold of 42°C for a minimum of 30 min, the tumor is destroyed.[42]

However, to date, most laboratory and animal model based studies have used magnetic field strengths that would have deleterious effects on humans, such as peripheral and skeletal muscle stimulation, cardiac stimulation, and arrhythmia and non-specific heating of tissue. This may be overcome by direct administration of the magnetic material directly into the target site rather than via the circulatory system. This would allow far greater quantities of the material to be used, and therefore, lower field strengths could be applied.

MRI Contrast Enhancement

Magnetic resonance imaging (MRI) utilizes the vast number of protons present in biological tissue as each has an extremely small magnetic moment, which together lead to a measurable response in a large magnetic field. The response is derived from the net magnetic moment of the protons in a radio frequency transverse field applied in a pulsed sequence. Pick-up coils within the MRI scanner measure induced currents caused by the relaxation of the response from the instant when the pulse is switched off.

By using magnetic contrast agents, the relaxation times T_1 (longitudinal or spin–lattice) and T_2 (transverse or spin–spin) can be shortened. Paramagnetic gadolinium ion complexes are the most commonly used contrast agents, while superparamagnetic (SPM) iron oxide particles are available for the organ specific targeting of liver lesions. In the field strengths normally used in MRI scanners, SPM particles become magnetically saturated, leading to a considerable locally perturbing dipolar field, which has the effect of shortening the relaxation times.

Magnetic nanoparticles are selectively taken up by the reticuloendothelial system of cells lining blood vessels, which remove foreign substances from the body, the differential up-take of different tissues in the body is vital for MRI.[43] Particle size is also of great importance; smaller particles have a longer half life in the blood stream, accumulating in the reticuloendothelial cells throughout the body.[44,45] One of the drawbacks of using iron oxide nanoparticles as contrast agents is their relatively low saturation magnetization, requiring the use of larger particles. Transition metal nanoparticles, e.g., those made from cobalt, have a much higher saturation magnetization value, allowing the use of smaller particles (<8 nm), without compromising sensitivity, and research is currently ongoing to assess their effectiveness.

CONCLUSIONS

We have attempted to present an up-to-date review of the synthesis, characterization, and biological application of magnetic nanoparticles. The synthetic methods currently used have to surmount the problem of producing particles that are not only soluble in aqueous solution but also able to withstand the specific environments present in a biological system (e.g., powerful electrolytes, etc.). Nanoparticles can be produced in aqueous solution, but tend to be polydisperse aggregates, whilst those produced in organic solvent are monodispersed but they do not readily dissolve in aqueous solution. In the future, new syntheses methods need to be developed that are designed with a specific biological application as the focus to overcome the problem of technology transfer as this is one of the major challenges in the biomedical application of magnetic nanoparticles.

ACKNOWLEDGMENTS

The authors thank the Royal Society, the EPSRC, and the North West Cancer Research fund for financial support. They also thank Drs. J. Goff, S. Lee, A. Cervellino, P. Murray, I. Prior, L. Parkes, R. Hodgson, and Professors D. Walton, D. Fernig, P. Rudland, and D. Edgar for their collaborative research and useful discussion.

REFERENCES

1. Tartaj, P.; Morales, M.P.; Veintemillas-Verdaguer, S.; Gonzalez-Carreno, T.; Serna, C.J. *Handbook of Magnetic Materials*; Elsevier: Amsterdam, 2006; 403–482.
2. Morales, M.P.; Gonzalez-Carreno, T.; Serna, C.J. The formation of alpha-Fe_2O_3 monodispersed particles in solution. J. Mater. Res. **1992**, *7*, 2538–2545.
3. Ocana, M.; Rodriguezclemente, R.; Serna, C.J. Uniform colloidal particles in solution—formation mechanisms. Adv. Mater. **1995**, *7*, 212–216.
4. Goia, D.V. Preparation and formation mechanisms of uniform metallic particles in homogeneous solutions. J. Mater. Chem. **2004**, *14*, 451–458.
5. Sun, S.H.; Anders, S.; Thomson, T.; Baglin, J.E.E.; Toney, M.F.; Hamann, H.F.; Murray, C.B.; Terris, B.D. Controlled synthesis and assembly of FePt nanoparticles. J. Phys. Chem. B **2003**, *107*, 5419–5425.
6. Chinnasamy, C.N.; Jeyadevan, B.; Shinoda, K.; Tohji, K. Polyol-process-derived CoPt nanoparticles: structural and magnetic properties. J. Appl. Phys. **2003**, *93*, 7583–7585.
7. Park, J.I.; Cheon, J. Synthesis of ''solid solution'' and ''core-shell'' type cobalt-platinum magnetic nanoparticles via transmetalation reactions. J. Am. Chem. Soc. **2001**, *123*, 5743–5746.
8. Park, J.I.; Kim, M.G.; Jun, Y.W.; Lee, J.S.; Lee, W.R.; Cheon, J. Characterization of superparamagnetic ''core-shell'' nanoparticles and monitoring their anisotropic phase transition to ferromagnetic ''solid solution'' nanoalloys. J. Am. Chem. Soc. **2004**, *126*, 9072–9078.
9. Lee, W.R.; Kim, M.G.; Choi, J.R.; Park, J.I.; Ko, S.J.; Oh, S.J.; Cheon, J. Redox-transmetalation process as a generalized synthetic strategy for core-shell magnetic nanoparticles. J. Am. Chem. Soc. **2005**, *127*, 16,090–16,097.
10. Pileni, M.P. Reverse micelles as microreactors. J. Phys. Chem. **1993**, *97*, 6961–6973.
11. Carpenter, E.E.; Sangregorio, C.; O'Connor, C.J. Effects of shell thickness on blocking temperature of nanocomposites of metal particles with gold shells. IEEE Trans. Magnetics **1999**, *35*, 3496–3498.
12. Lin, J.; Zhou, W.L.; Kumbhar, A.; Wiemann, J.; Fang, J.Y.; Carpenter, E.E.; O'Connor, C.J. Gold-coated iron (Fe@Au) nanoparticles: synthesis, characterization, and magnetic field-induced self-assembly. J. Solid State Chem. **2001**, *159*, 26–31.
13. Cho, S.J.; Idrobo, J.C.; Olamit, J.; Liu, K.; Browning, N.D.; Kauzlarich, S.M. Growth mechanisms and oxidation resistance of gold-coated iron nanoparticles. Chem. Mater. **2005**, *17*, 3181–3186.
14. Mikhaylova, M.; Kim, D.K.; Bobrysheva, N.; Osmolowsky, M.; Semenov, V.; Tsakalakos, T.; Muhammed, M. Superparamagnetism of magnetite nanoparticles: dependence on surface modification. Langmuir **2004**, *20*, 2472–2477.
15. Mandal, M.; Kundu, S.; Ghosh, S.K.; Panigrahi, S.; Sau, T.K.; Yusuf, S.M.; Pal, T. Magnetite nanoparticles with tunable gold or silver shell. J. Colloid Interface Sci. **2005**, *286*, 187–194.
16. Nayak, S.; Lyon, L.A. Soft nanotechnology with soft nanoparticles. Angewandte Chemie-International Edition **2005**, *44*, 7686–7708.
17. Kondo, A.; Kamura, H.; Higashitani, K. Development and application of thermosensitive magnetic immunomicrospheres for antibody purification. Appl. Microbiol. Biotechnol. **1994**, *41*, 99–105.
18. Puntes, V.F.; Krishnan, K.M.; Alivisatos, A.P. Colloidal nanocrystal shape and size control: the case of cobalt. Science **2001**, *291*, 2115–2117.
19. Ma, W.W.; Yang, Y.; Chong, C.T.; Eggeman, A.; Piramanayagam, S.N.; Zhou, T.J.; Song, T.; Wang, J.P. Synthesis and magnetic behavior of self-assembled Co nanorods and nanoballs. J. Appl. Phys. **2004**, *95*, 6801–6803.
20. Stevenson, J.P.; Rutnakornpituk, M.; Vadala, M.; Esker, A.R.; Charles, S.W.; Wells, S.; Dailey, J.P.; Riffle, J.S. Magnetic cobalt dispersions in poly-(dimethylsiloxane) fluids. J. Magn. Magn. Mater. **2001**, *225*, 47–58.
21. Thanh, N.T.K.; Puntes, V.F.; Tung, L.D.; Fernig, D.G. Peptides as capping ligands for *in situ* synthesis of water soluble Co nanoparticles for bioapplications. J. Phys.: Confer. Ser. **2005**, *17*, 70–76.
22. Hyeon, T.; Lee, S.S.; Park, J.; Chung, Y.; Bin Na, H. Synthesis of highly crystalline and monodisperse maghemite nanocrystallites without a size-selection process. J. Am. Chem. Soc. **2001**, *123*, 12798–12801.
23. Park, J.; Lee, E.; Hwang, N.M.; Kang, M.S.; Kim, S.C.; Hwang, Y.; Park, J.G.; Noh, H.J.; Kim, J.Y.; Park, J.H.; Hyeon, T. One-nanometer-scale size-controlled synthesis of monodisperse magnetic iron oxide nanoparticles. Angewandte Chemie-International Edition **2005**, *44*, 2872–2877.
24. Wang, L.Y.; Luo, J.; Fan, Q.; Suzuki, M.; Suzuki, I.S.; Engelhard, M.H.; Lin, Y.H.; Kim, N.; Wang, J.Q.; Zhong, C.J. Monodispersed core-shell Fe_3O_4@Au nanoparticles. J. Phys. Chem. B **2005**, *109*, 21, 593–21, 601.
25. Tartaj, P.; Morales, M.D.; Veintemillas-Verdaguer, S.; Gonzalez-Carreno, T.; Serna, C.J. The preparation of magnetic nanoparticles for applications in biomedicine. J. Phys. D-Appl. Phys. **2003**, *36*, R182–R197.
26. Ocana, M.; Morales, M.P.; Serna, C.J. The growth-mechanism of alpha-Fe_2O_3 ellipsoidal particles in solution. J. Colloid Interface Sci. **1995**, *171*, 85–91.
27. Gee, S.H.; Hong, Y.K.; Erickson, D.W.; Park, M.H.; Sur, J.C. Synthesis and aging effect of spherical magnetite (Fe_3O_4) nanoparticles for biosensor applications. J. Appl. Phys. **2003**, *93*, 7560–7562.
28. Si, S.; Kotal, A.; Mandal, T.K.; Giri, S.; Nakamura, H.; Kohara, T. Size-controlled synthesis of magnetite nanoparticles in the presence of polyelectrolytes. Chem. Mater. **2004**, *16*, 3489–3496.
29. Rietveld, H.M. A profile refinement method for nuclear and magnetic structures. J. Appl. Crystallography **1969**, *2*, 65–71.
30. Rodriguez-Carvajal, J. FullProf: a program for rietveld refinement and profile matching analysis of complex powder diffraction patterns (ILL, unpublished).

31. Klug, H.P.; Alexander, L.E. X-ray diffraction procedures for polycrystalline and amorphous materials, 2nd Ed.; Wiley-Interscience: New York, 1974.
32. Tung, L.D.; Kolesnichenko, V.; Caruntu, D.; Chou, N.H.; O'Connor, C.J.; Spinu, L. Magnetic properties of ultrafine cobalt ferrite particles. J. Appl. Phys. **2003**, *93*, 7486–7488.
33. Johnson, C.E. Characterization of magnetic materials by Mössbauer spectroscopy. J. Phys. D. Appl. Phys. **1996**, *29*, 2266–2273.
34. Bellouard, C.; Mirebeau, I.; Hennion, M. Magnetic correlations of fine ferromagnetic particles studied by small-angle neutron scattering. Phys. Rev. B **1996**, *53*, 5570–5578.
35. Ijiri, Y.; Kelly, C.V.; Borchers, J.A.; Rhyne, J.J.; Farrell, D.F.; Majetich, S.A. Detection of spin coupling in iron nanoparticles with small angle neutron scattering. Appl. Phys. Lett. **2005**, *86*, 243102.
36. Schutt, W.; Gruttner, C.; Hafeli, U.; Zborowski, M.; Teller, J.; Putzar, H.; Schumichen, C. Applications of magnetic targeting in diagnosis and therapy—possibilities and limitations: a mini-review. Hybridoma **1997**, *16*, 109–117.
37. Alexiou, C.; Arnold, W.; Klein, R.J.; Parak, F.G.; Hulin, P.; Bergemann, C.; Erhardt, W.; Wagenpfeil, S.; Lubbe, A.S. Locoregional cancer treatment with magnetic drug targeting. Can. Res. **2000**, *60*, 6641–6648.
38. Lubbe, A.S.; Bergemann, C.; Brock, J.; McClure, D.G. Physiological aspects in magnetic drug-targeting. J. Magn. Magn. Mater. **1999**, *194*, 149–155.
39. Mehta, R.V.; Upadhyay, R.V.; Charles, S.W.; Ramchand, C.N. Direct binding of protein to magnetic particles. Biotechnol. Techniques **1997**, *11*, 493–496.
40. Koneracka, M.; Kopcansky, P.; Antalik, M.; Timko, M.; Ramchand, C.N.; Lobo, D.; Mehta, R.V.; Upadhyay, R.V. Immobilization of proteins and enzymes to fine magnetic particles. J. Magn. Magn. Mater. **1999**, *201*, 427–430.
41. Koneracka, M.; Kopcansky, P.; Timko, M.; Ramchand, C.N.; de Sequeira, A.; Trevan, M. Direct binding procedure of proteins and enzymes to fine magnetic particles. J. Mol. Catal. B-Enzymatic **2002**, *18*, 13–18.
42. Pankhurst, Q.A.; Connolly, J.; Jones, S.K.; Dobson, J. Applications of magnetic nanoparticles in biomedicine. J. Phys. D-Appl. Phys. **2003**, *36*, R167–R181.
43. Lawaczeck, R.; Bauer, H.; Frenzel, T.; Hasegawa, M.; Ito, Y.; Kito, K.; Miwa, N.; Tsutsui, H.; Volger, H.; Weinmann, H.J. Magnetic iron oxide particles coated with carboxydextran for parenteral administration and liver contrasting—Pre-clinical profile of SH U555A. Acta Radiologica **1997**, *38*, 584–597.
44. Weissleder, R.; Elizondo, G.; Wittenberg, J.; Rabito, C.A.; Bengele, H.H.; Josephson, L. Ultrasmall superparamagnetic iron-oxide—characterization of a new class of contrast agents for MR imaging. Radiology **1990**, *175*, 489–493.
45. Ruehm, S.G.; Corot, C.; Vogt, P.; Kolb, S.; Debatin, J.F. Magnetic resonance imaging of atherosclerotic plaque with ultrasmall superparamagnetic particles of iron oxide in hyperlipidemic rabbits. Circulation **2001**, *103*, 415–422.